

UDC 550.388.2

S. V. GRINCHENKO, scientific researcher, Institute of Ionosphere, Kharkiv**SEASONAL ANOMALY IN VARIATIONS OF GLOBAL DISTRIBUTIONS OF F2-LAYER ELECTRON DENSITY ACCORDING TO CCIR MODEL**

There are presented the global distributions of electron density $n_{e\max}F2$ and height $h_{\max}F2$ of the main maximum of ionosphere. There are analyzed the basic regularities of longitude-latitudinal variations of these parameters in the northern and southern hemispheres. The main attention is given to the effect of seasonal anomaly. It is shown that, according to calculations by the CCIR model seasonal anomaly appears at latitudes between 15 and 60 degrees N. approximately from 9 to 12 hours of local time. In the southern hemisphere the seasonal anomaly is not observed.

Keywords: CCIR model, IRI, NeQuick model, global distribution of ionospheric parameters, geographical anomaly, seasonal anomaly, December anomaly, semiannual anomaly, Visual Fortran.

Statement of the problem. CCIR model of the distribution of electron density and height of F2-layer is constructed according to the data of the global network of vertical sounding stations. It is the basic empirical model of main maximum parameters of the quiet ionosphere. CCIR model allows to make daily calculations during various seasons at different levels of solar activity. The analysis of seasonal variations of F2-layer parameters according to CCIR model is important for confirmation of the results of theoretical simulation of quiet ionosphere parameters (electron density, transport plasma velocity, ion and electron temperatures) and comparisons with the incoherent scatter data. The main goal of this research is to construct global distribution of the main maximum parameters of the ionospheric plasma and to identify manifestations of seasonal anomalies and other features of the F2-layer morphology in longitude-latitudinal distributions of the northern and southern hemispheres.

The review of known anomalies of F2-layer morphology. F2-region (≈ 210 -500 km) is the most difficult ionosphere area from the point of view of morphology of daily and seasonal variations of electron density altitude profile. The major ions in this region are the atomic nitrogen N^+ and atomic oxygen O^+ with a strong predominance of oxygen ions. Although the ion composition of F2-region is not complex, the electron density and height of layer F2 vary with complexity. It is a result of the dynamic processes peculiar to this area. Dynamic processes are determined by ambipolar diffusion and motion of ions and electrons in the magnetic and electric fields in the environment of horizontally moving neutral particles.

The behavior of F2-layer isn't described even in the first approximation by the theory of the Chapman layer. The regularities of F2-layer morphology which

© S. V. Grinchenko, 2014

don't keep within simple relations of Sun arrangement in the dome of the sky and values of maximum electron density and height of the F2-layer in the framework of Chapman theory are conventionally called "anomalies". The variations in the course of any year or day, changes with latitude are anomalous too.

The daily course of the electron density at F2-layer maximum is called anomalous, since diurnal variations can have one or two minima and one or two maxima, and the main maximum can be shifted relative to the noontime for a few hours (daily anomaly).

Geographical anomaly is manifested in the fact that the electron density maximum throughout the year shifts to the north of the geographic equator. Geographic anomaly is observed not only in the vernal and autumnal equinoxes, and even in the winter solstice.

It is accepted to understand the phenomenon of excess of winter day values of electron density $n_{e\ max}F2$ in maximum of layer over the summer ones as seasonal anomaly of F2-layer. The extent of this excess, as well as the behavior of other layer parameters – maximum height $h_{max}F2$, the upper and lower semithicknesses of the layer – are various for different geographic coordinates and levels of solar activity.

December anomaly is that in the range of the northern mid-latitudes to the southern mid-latitudes day values of electron density $n_{e\ max}F2$ are anomalously high in November, December and January. December anomaly strengthens seasonal one at northern mid-latitudes.

Also it is possible to note semiannual anomaly: during equinox periods day values of electron density are comparable with winter values (and hence exceed summer values).

General information about CCIR model. The full name of this model – CCIR f_0F2 and M(3000)F2 Model Maps 1982. Abbreviation CCIR is the reduced name of the International Radio Consultative Committee. The International Radio Consultative Committee was established in 1927. In 1992 the CCIR has been converted into Radiocommunication Sector of the International Telecommunication Union. The International Telecommunication Union (ITU) is a specialized agency of the United Nations Organization on information and communication technologies. The ITU Radiocommunication Sector (ITU-R) publishes regulations, recommendations, reports and handbooks compiled by research groups on a radio communication. In the ITU-R documents CCIR model is recommended for calculation of parameters of the F2-layer at modelling of radio paths [10].

CCIR model contains a set of coefficients f_0F2 and M(3000)F2, allowing to calculate the ionospheric F2-layer parameters. Both parameters f_0F2 and M(3000)F2 are read from ionograms.

Propagation factor M(3000)F2=MUF(3000)/ f_0F2 . MUF(3000) is a maximum usable frequency, reflected from the F2 layer with a height of 3000 km.

The CCIR maps are received by the average values of a worldwide network of ionosondes. Mathematical bases of numerical methods used in the description of daily and geographic variations of these parameters are described in the papers by William B. Jones [1, 2]. At first, the data set of each station is represented by time Fourier series (in Universal Time). For according to the geographical latitude and longitude each Fourier coefficient is represented as a decomposition using Legendre functions. Series coefficients are calculated for the high and low solar activity. For intermediate levels of solar activity linear interpolation is used.

Database CCIR, currently known as a database ITU-R [10], consists of 12 files (on one for each month of the year). Files contains the coefficients needed to describe the time and geographical variations of the values $M(3000)F_2$ and f_oF_2 . Each file contains: 1) 882 coefficients for $M(3000)F_2$ (441 – for solar activity at Wolf number $W=0$ and 441 – for solar activity at $W=100$); 2) 1976 coefficients for f_oF_2 (988 – for $W=0$ and 988 – for $W=100$). Thus, the whole CCIR model consists of $(441+988) \cdot 2 \cdot 12 = 34,296$ coefficients.

Critical frequency of the electromagnetic wave reflected from the layer of electron density $f_0^2 = \frac{e^2 n_{e \max}}{\pi m_e}$. From here the maximum of electron density in layer expresses as $n_{e \max} = \frac{\pi m_e}{e^2} f_0^2$.

Considering, that $m_e = 9.1095 \cdot 10^{-28} \text{ g}$, $e = 4.8034 \cdot 10^{-10} \text{ abstat unit}$, we receive $\frac{\pi m_e}{e^2} = \frac{\pi \cdot 9.1095 \cdot 10^{-28}}{(4.8034)^2 \cdot 10^{-20}} = 1.2404 \cdot 10^{-8} \frac{\text{g}}{(\text{abstat unit})^2}$.

If critical frequency f_0 is measured in MHz, and electron density concentration – in sm^{-3} , then $n_{e \max} = 1.2404 \cdot 10^{-8} \cdot 10^{12} \cdot f_0^2 = 1.2404 \cdot 10^4 \cdot f_0^2$, $\lg n_{e \max} = \lg 1.2404 + 4 + 2 \cdot \lg f_0 = 4.0936 + 2 \cdot \lg f_0$. The square of critical frequency $f_0^2 = \frac{10^{-4}}{1.2404} \cdot n_{e \max} = 8.0619 \cdot 10^{-5} \cdot n_{e \max}$.

There are constantly improving techniques that allow on the critical frequency and f_oF_2 propagation constant $M(3000)F_2$ to calculate the height $h_{\max}F_2$ of the layer maximum F2 [3, 4, 5].

Comparisons of the planetary distributions of F2-layer parameters calculated from the empirical CCIR model and from theoretical calculations have shown a consistency of the general character of longitude-latitudinal variations [6, 7].

In spite of the continuously improvement of coefficient arrays with using of new ionospheric data [8, 9, 10], the same coefficient arrays of version 1982 are

applied in NeQuick model and in all versions of IRI model (from IRI-1990 to IRI-2011) presented on the Internet for free using.

Formulas of planetary distribution of f_0F_2 , M(3000)F₂. To describe the global distribution of time dependences of ionospheric characteristics f_0F_2 , M(3000)F₂ in CCIR model [10] it is used the time series Fourier which coefficients are expanded in spherical Legendre functions:

$$\Omega(\varphi, \lambda, T) = a_0(\varphi, \lambda) + \sum_{i=1}^6 [a_i(\varphi, \lambda) \cos(iT) + b_i(\varphi, \lambda) \sin(iT)],$$

where Ω – ionospheric characteristics f_0F_2 , M(3000)F₂; φ – geographic latitude ($-90^\circ \leq \varphi \leq 90^\circ$); λ – geographic longitude ($0^\circ \leq \lambda \leq 360^\circ$); T – Coordinated Universal Time (UTC), presented in the form of an angle ($0^\circ \leq T \leq 360^\circ$).

Expansion coefficients in the Fourier series on variable T are represented as:

$$a_i(\varphi, \lambda) = \sum_{k=0}^{75} U_{2i,k} G_k(\varphi, \lambda) \quad (i = \overline{0,6}),$$

$$b_i(\varphi, \lambda) = \sum_{k=0}^{75} U_{2i-1,k} G_k(\varphi, \lambda) \quad (i = \overline{1,6}),$$

where $G_k(\varphi, \lambda)$ – spherical Legendre functions.

Thus, the numerical mapping function that describes the global distribution of ionospheric characteristics f_0F_2 , M(3000)F₂, can be written as:

$$\begin{aligned} \Omega(\varphi, \lambda, T) = & \sum_{k=0}^{75} U_{0,k} G_k(\varphi, \lambda) + \\ & + \sum_{i=1}^6 \left[\cos(iT) \sum_{k=0}^{75} U_{2i,k} G_k(\varphi, \lambda) + \sin(iT) \sum_{k=0}^{75} U_{2i-1,k} G_k(\varphi, \lambda) \right]. \end{aligned}$$

Since CCIR files contain values f_0F_2 , M(3000)F₂ for two levels of solar activity, characterized by Wolf indices $W=0$ and $W=100$, the series expansion is carried out twice.

Remarks on the relationship of local time LT and Coordinated Universal Time UTC, used in the CCIR model. At the simulation of ionospheric processes it is convenient to use time directly connected with Sun hour angle t . For the zenith angle z , which determines the intensity of the ionizing radiation of the Sun, we have the formula: $\cos z = \sin \varphi \cdot \sin \delta + \cos \varphi \cdot \cos \delta \cdot \cos t$, where φ – latitude of the observation point, δ – declination of the Sun. The hour corner of the Sun $t = 15^\circ (LT - LT_0)$, where LT – local time; at the moment of LT_0 the Sun is in upper culmination point, crossing the meridian of the observation point. Since the local time is determined by the Sun position, it is also called solar time.

Because of the Earth's orbit ellipticity the linear velocity of movement and the angular velocity of rotation of the Earth around the Sun varies throughout the

year. The Earth moves most slowly on its orbit, while it is at aphelion – the farthest point from the Sun, and most fast – while at perihelion. This is the significant cause of change in the duration of solar day during a year.

At apparent local time $LT=12.00$ the Sun is in the top culmination point. Since the duration of a day varies throughout a year, the researches use the mean solar day, tied to the so-called average Sun – a conditional point moving in regular intervals along the celestial equator (instead of on ecliptic, as the real Sun) and coinciding with the center of the Sun at the vernal equinox. There is a system of readout of average local time. Average local time of the upper culmination varies during a year approximately from 11 h 45 min to 12 h 15 min.

Further we will use the average local time, calling it for short as local time. The local time (so we have agreed to call the average local time) of Greenwich meridian is Greenwich Mean Time (GTM).

There are various versions of universal time based on the rotation of the Earth relative to distant celestial objects (stars and quasars). The universal time UT1 is a basic version of a universal time. UT1 is calculated proportional to the angle of rotation of the Earth relative to the International Celestial Reference System (ICRS). The Coordinated Universal Time (UTC) is a time scale approximating UT1. UTC goes synchronously with the International Atomic Time (TAI).

Usually a UTC day consist 86,400 SI seconds. However for maintenance of divergence UTC and UT1 no more than 0.9 seconds with necessary of June, 30th or on December, 31st an additional second of coordination is added or subtracted. Besides the listed versions of universal time there are also others: UT0, UT1R, UT2, UT2R.

For ionospheric simulation differences between varioust versions of Universal Time and Greenwich Mean Time are insignificant. Therefore the local time on the zero meridian is assumed to be equal to a “certain” universal time. And as a universal time for ionospheric calculations it is possible to take any version of Universal Time.

The review of empirical models of altitude profiles of ionospheric parameters using CCIR model for calculation of F2-layer parameters. There are widely known the empirical model of ionosphere IRI (Fortran codes of various versions are on the NASA site), the European empirical model NeQuick (Fortran code can be found in the section of the free software of site ITU-R), the empirical model SPIM (Standard Ionosphere and Plasmasphere Model), codes various versions of which are available for public using on the IZMIRAN site. All of these programs to calculate electron density and height of the F2 maximum use CCIR model.

For using CCIR model in NeQuick it is necessary to input geographical longitude and latitude, number of month, Covington index $F_{10.7}$ and universal time.

For using CCIR model in IRI instead of a number of month it is necessary to input the concrete date (number and month) or corresponding number of day in a year. The IRI model has an interpolating dependence of monthly calculations, allowing to set not only a number of month, but also a number of day of the concrete month. The activity index $F_{10.7}$ is replaced by Wolf number W . These indexes are connected by the certain known dependence and easily recalculated into each other.

For values $W \leq 150$ and $F_{10.7} \leq 192.975$ the IRI model uses the following ratio: $F_{10.7} = 63.75 + W \cdot (0.728 + 0.00089 \cdot W)$.

And so, $0.00089 \cdot W^2 + 0.728 \cdot W - (F_{10.7} - 63.75) = 0$,

$$W = 33.5201 \cdot \sqrt{F_{10.7} + 85.122} - 408.989 = \\ = \sqrt{167271.8 + 1123.596 \cdot (F_{10.7} - 63.75)} - 408.989.$$

Value of $W = 11$ corresponds to $F_{10.7} = 71.87$. Value $F_{10.7} = 70$ corresponds to $W = 8.50$, and the value of $F_{10.7} = 100$ corresponds to $W = 47.08$.

The global longitude-latitudinal variations of electron density and height of the F2-layer maximum. To research the behavior of the maximum electron density $n_{e \max} F2$ and height $h_{\max} F2$ we'll build the longitude-latitudinal distribution of these values along the northern and southern hemispheres. Calculation of the electron density and height of the F2 layer are carried by CCIR model.

Figures 1-9 show the distributions of the decimal logarithm of electron density at the F2-layer maximum, measured in cm^{-3} . For the better perception of figures on schematic maps of hemispheres contours of continents and large islands are plotted. There are marked latitudes in 30 and 60 degrees and longitudes from 0 to 360 degrees with the step of 30 degrees.

To the each global distribution there corresponds some value of universal time UT. For example, at UT=0 local time LT for zero longitude equals 0 too. Through every 30 degrees for each of the 12 plotted longitudes there added 2 hours of local time.

On the northern hemispheres the point designates the location of the Kharkov Incoherent Scatter Radar. When universal time is 12 hours, at the Radar there is a little more than 14 hours of local time.

The presented figures are executed by programming in Visual Fortran language.

Before to analyze the manifestations of seasonal anomaly on the global distributions of electron density, there is of interest to dwell on an asymmetry of electron density distribution about rotation axis (i.e. the axis passing through the geographical poles).

Figures 1 and 2 show the $\lg n_{e \max} F2$ December distributions in Covington index 71.87, and UT = 0, 12 respectively.

The axial asymmetry is the result of a mismatch of the Earth magnetic field poles with the geographic ones. Difference in geometry of the magnetic field lines relative to the geographical meridians, for example, in the North American and the European regions, leads to some quantitative differences of electron density variations. At a generality of physics of a middle-latitude ionosphere the ionosphere morphology in these regions has quantitative differences.

In both figures at middle latitudes there are well visible regions of the lowered $n_{e\max}F2$ values in the morning and evening hours, corresponding to minima in the winter daily course. Around 12-14 hours of local time in both figures there is observed the maximum of F2-layer electron density.

The global distribution of F2-layer seasonal anomaly. The seasonal anomaly of electron density is illustrated in figure 2 and 3. The December distribution is characterized by high-amplitude variations of the electron density. If at night electron density in December is less, than in June, then at the mid-latitudes December daily values of electron density there are more than June ones. In winter at mid-latitudes daytime electron density at the F2-layer maximum is greater than the summer values. The effect of seasonal anomalies is observed, as seen from the figures, in the period 12-14 LT in the latitude range about from 15° to 60° N.

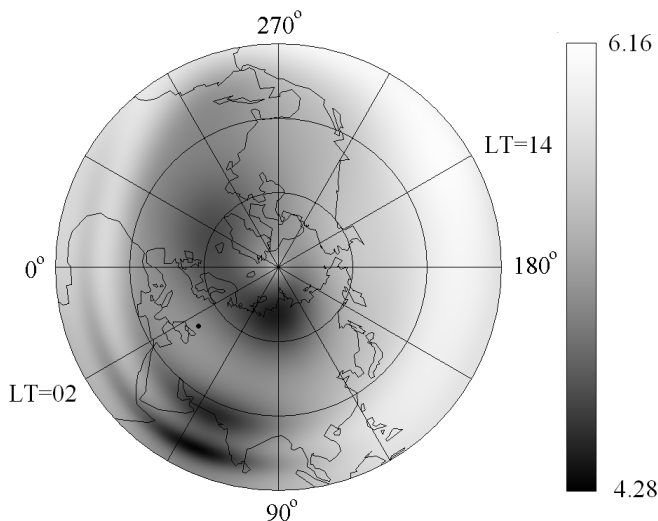


Fig. 1 – The December $\lg n_{e\max}F2$ distribution for northern hemisphere (UT = 00).
The minimum value of $\lg n_{e\max}F2$ equals 4.31, maximum – 6.13.

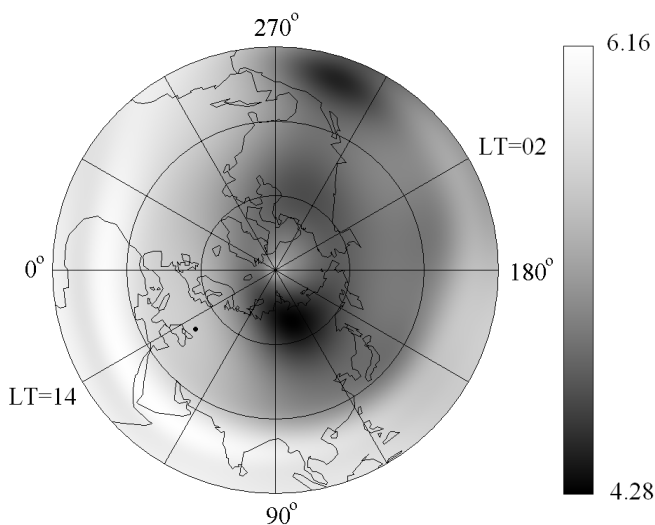


Fig. 2 – The December $\lg n_{e \max} F2$ distribution for northern hemisphere (UT=12).
The minimum value of $\lg n_{e \max} F2$ equals 4.28, maximum – 6.16.

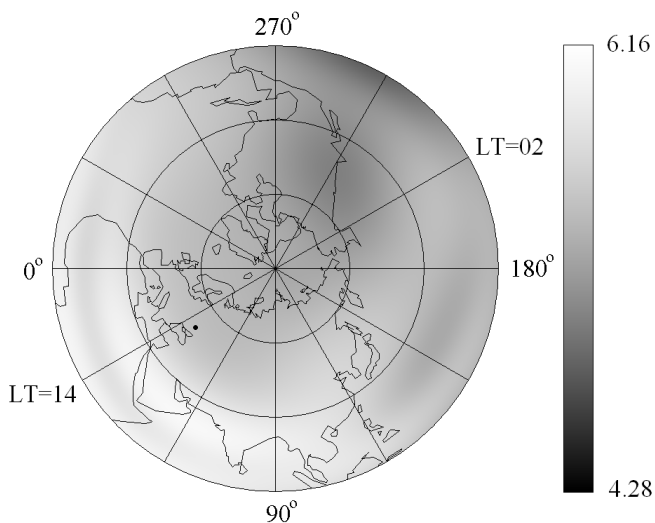


Fig. 3 – The June $\lg n_{e \max} F2$ distribution for northern hemisphere (UT=12).
The minimum value of $\lg n_{e \max} F2$ equals 4.79, maximum – 6.07.

The sharper changes of electron density of the main maximum are observed during winter time in comparison with summer time. This is also true for the southern hemisphere in the conditions of local winter and local summer.

In southern hemisphere (fig. 4, 5) the phenomenon of seasonal anomaly is absent. In the southern hemisphere there is excess of electron density during the local summer over the winter ones in almost all latitudes and longitudes.

Naturally, in June the electron density values of the northern hemisphere is greater than values in the southern hemisphere. In December in the southern hemisphere it is so-called local summer, and the electron density values of the southern hemisphere is greater than values of the northern hemisphere.

Morphology of F2 maximum height. In northern hemisphere (fig. 6, 7) the summer values of F2-layer height are greater than the winter ones except for some equatorial regions. Calculations on CCIR model were made at $F_{10.7} = 71.87$.

The sharper changes of height of F2 maximum are observed in winter time in comparison with summer time. For local winter and local summer of the southern hemisphere this is also true.

In southern hemisphere (fig. 8, 9) the height of layer F2 in the conditions of local summer is more than values of this height in the conditions of local winter practically at all values of co-ordinates.

In the southern hemisphere (fig. 8, 9), the height of the F2 layer in the conditions of local summer is greater than the height at the local winter conditions practically at all coordinates.

Quite naturally, in June the F2-layer height in the northern hemisphere is greater than the height in the southern hemisphere. In December in the southern hemisphere in the conditions of the local summer the F2-layer height is greater than the height in the northern hemisphere.

Thus, we can say that the phenomenon of seasonal anomaly (excess of the winter values of electron density of the F2 layer over the summer ones) is observed only in the northern hemisphere at mid-latitudes. Under other conditions there are exceeded the summer values of electron density and height of the F2-layer over the winter ones. Some equatorial regions can be an exception.

The daily variations of electron density and height of maximum F2 over a point of a location of Kharkov Incoherent Scatter Radar. Fig. 10 shows the daily variations of the electron density and height of F2-layer in June and December at $F_{10.7}=72$. If at night the summer values of electron density exceeds the winter values than approximately from 10 to 16 of local time there is observed an anomalous excess of winter values of electron density on the summer ones. At night seasonal anomaly is not observed.

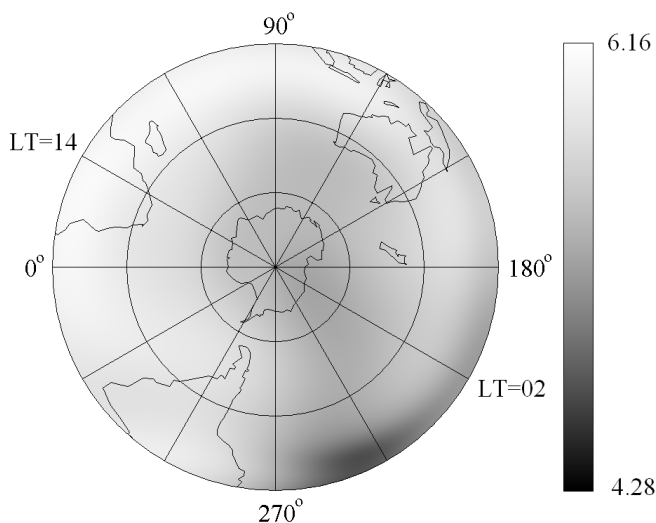


Fig. 4 – The December $\lg n_{e \max} F_2$ distribution of southern hemisphere in the conditions of local summer (UT=12). The minimum value of $\lg n_{e \max} F_2$ equals 4.69, maximum – 6.09.

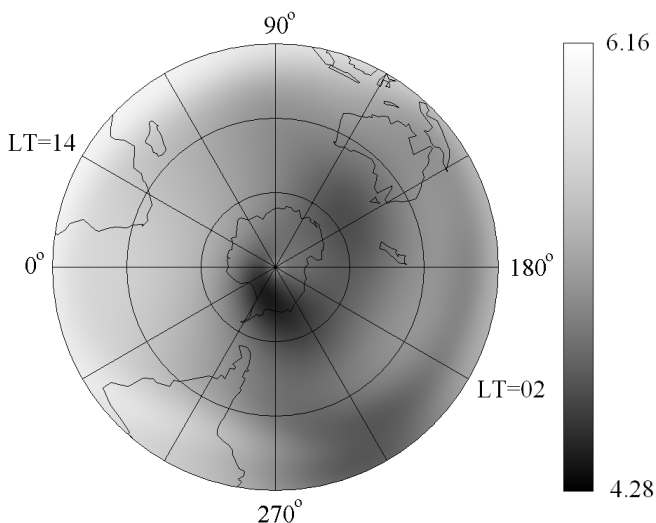


Fig. 5 – The June $\lg n_{e \max} F_2$ distribution of southern hemisphere in the conditions of local winter (UT=12). The minimum value of $\lg n_{e \max} F_2$ equals 4.41, maximum – 6.03.

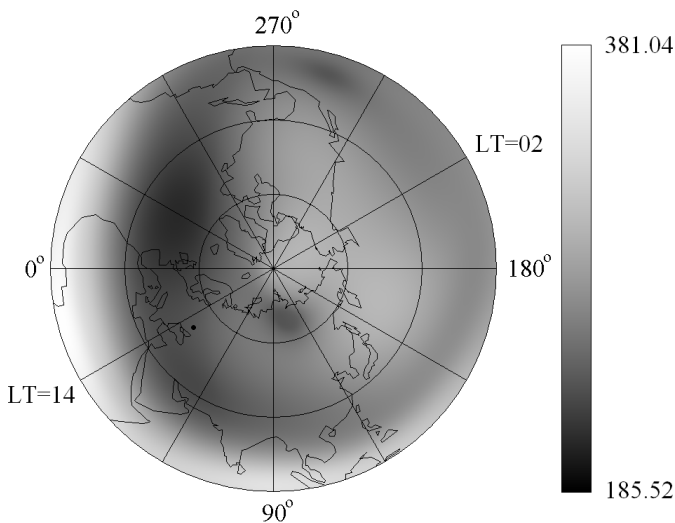


Fig. 6 – The December h_{\max} F2 distribution of northern hemisphere (UT=12). The minimum value of h_{\max} F2 equals 207.11 km, maximum – 381.04 km.

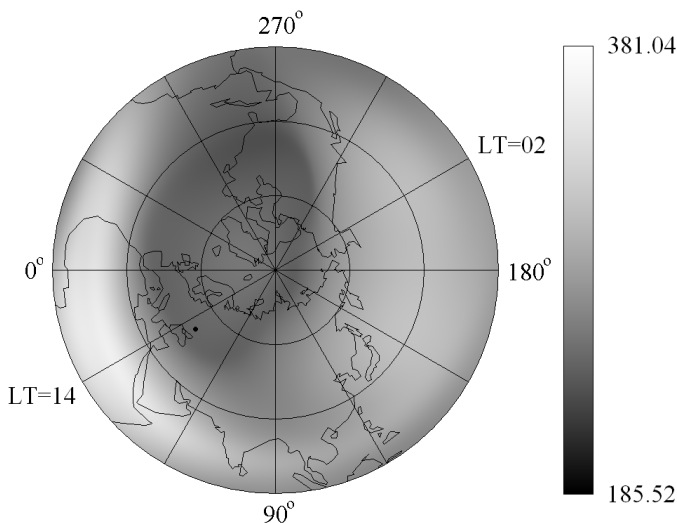


Fig. 7 – The June h_{\max} F2 distribution of northern hemisphere (UT=12). The minimum value of h_{\max} F2 equals 228.55 km, maximum – 360.84 km.

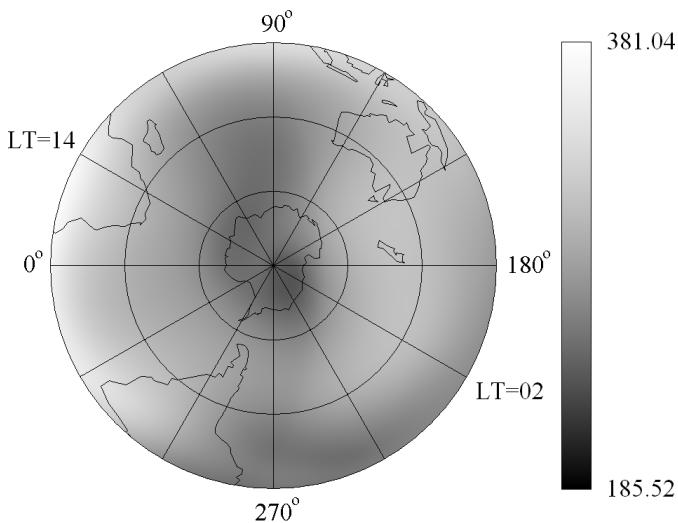


Fig. 8 – The December $h_{max}F_2$ distribution of southern hemisphere in the conditions of local summer (UT=12). The minimum value of $h_{max}F_2$ equals 231.96 km, maximum – 378.41 km.

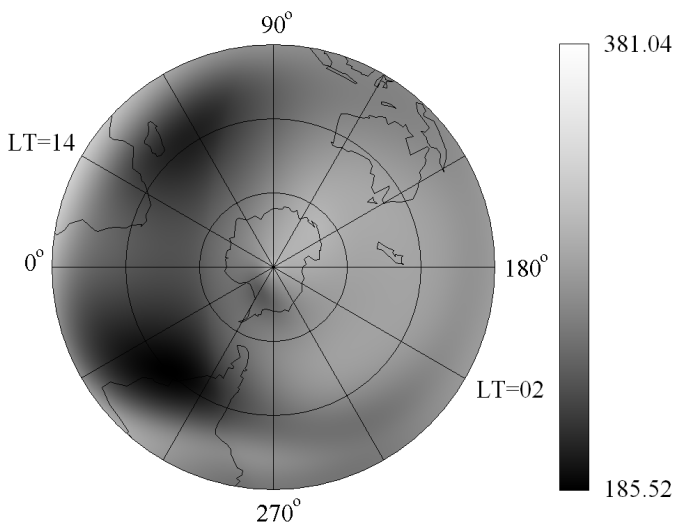


Fig. 9 – The June $h_{max}F_2$ distribution of southern hemisphere in the conditions of local winter (UT=12). The minimum value of $h_{max}F_2$ equals 185.52 km, maximum – 327.13 km.

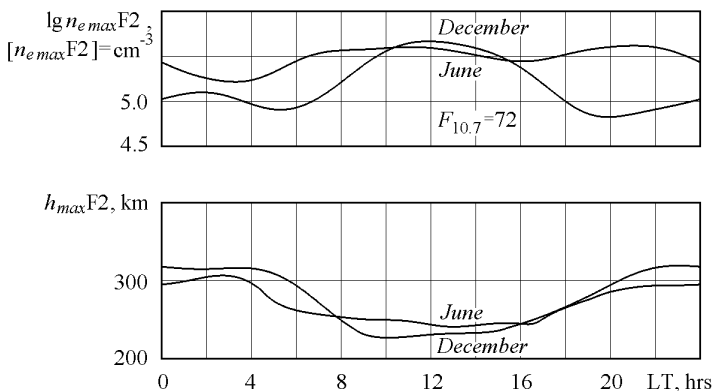


Fig. 10 – The daily variations of the electron density in the F2-layer maximum and maximum height above the point of a location of the Kharkov Incoherent Scatter Radar at $F_{10.7}=72$.

In the middle of June the sunrise time is about 4.6 LT, the sunset time – 20.8 LT. The sun doesn't disappear behind horizon approximately over 275 km. In the middle of December the Sun rises at $LT \approx 7.9$ and sets at $LT \approx 16.0$.

For winter the daily course is characterized by: 1) the considerable (to an order of values) variations of $n_{e \max} F2$; 2) the pronounced pre-sunrise minimum, the fast growth in the morning; 3) a maximum in a daily course about 12 LT; 4) the decline in the afternoon.

The fast growth of the electron density in winter in the morning after a minimum is accompanied by the further lowering of height of the layer maximum. The time interval of the least heights coincides with the time interval of the maximum values of electron density. After this the layer F2 begins to rise. The greatest height of the layer is observed around midnight.

An interesting feature of the behavior of the winter ionosphere at middle latitudes is a night increase of electron density.

The summer type of daily variations is characterized by: 1) the inconsiderable daily variations (the diurnal values approximately twice more the night ones); 2) poorly expressed minimum at pre-sunrise time; 3) the presence of two maxima in a daily $n_{e \max} F2$ course (day maximum – about 11 LT and evening one – about 21 LT; 4) the after-sunset decreasing of electron density until sunrise.

Fig. 11 shows the daily variations at higher solar activity (Covington index $F_{10.7}=100$). The seasonal anomaly is manifested already in a larger time interval – from 9 to 17 local time and not from 10 to 16, as in the previous case.

It should be noted a common pattern of change of electron density and height of the F2-layer maximum: an increase of electron density is almost always connected with a decrease of height of the layer and vice versa.

As it has been noted, the effect of seasonal anomaly of electron density is more expressed at higher solar activity (SA). This is due to the fact that although both in winter and summer at an increase of solar activity there are observed an increase of height of the layer and electron density during the whole day (figure 12, 13), the increase of electron density is more considerable during the winter daytime in comparison with summer increase.

The changes in solar activity does not affect the nature of the daily variations. A number of maxima and minima of the daily course remains invariable at SA changing. The moments of extrema of daily course of $n_{e\max}F2$ and $h_{\max}F2$ do not change with SA increasing.

Against the comparison of the daily courses in June and December it is represented interesting to compare the daily variations of electron density and height of F2-layer in March and September.

In the middle of March the sunrise time is about 6.3 LT, the sunset time – 18.0 LT. In the middle of September the Sun rises at LT \approx 5.6 and sets at LT \approx 18.2.

Although the March daytime values of electron density exceed September ones a little, the daily courses of electron density are generally similar. Also the daily courses of height of F2-layer are close. Thus, the spring and autumn variations of electron density and height of F2 maximum are approximately identical.

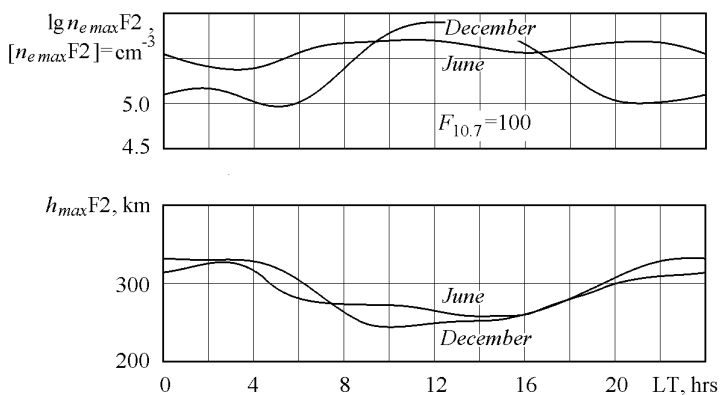


Fig. 11 – The daily variations of the electron density in the F2-layer maximum and maximum height above the point of a location of the Kharkov Incoherent Scatter Radar at $F_{10.7}=100$.

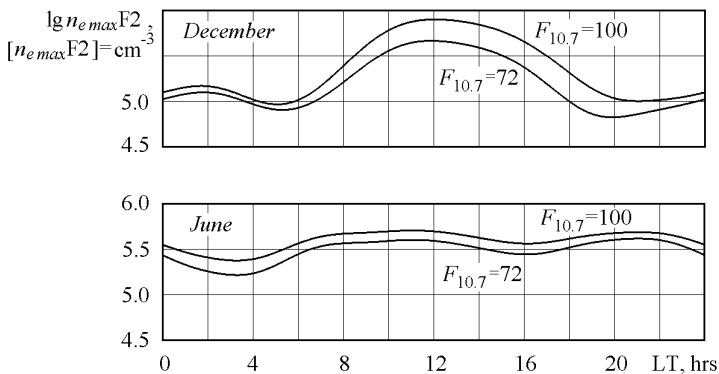


Fig. 12 – Increase of electron density of F2-layer at increasing of solar activity

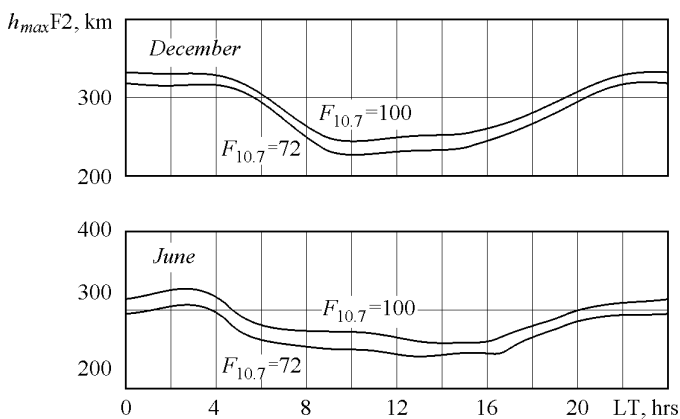


Fig. 13 – Increase of height of layer F2 at increase of solar activity

The daily variations of electron density and height of F2-layer maximum at mid-latitudes of the southern hemisphere. In the southern hemisphere the phenomenon of seasonal anomaly is absent: there is the excess of the local summer values of electron density over the electron density values in conditions of local winter practically at all latitudes and longitudes. This can be illustrated with fig.15 for 49.7° latitude south of the equator unlike northern latitude 49.7° of Kharkov Incoherent Scatter Radar used in the previous calculations. A comparison of the winter and summer variations do not carry in the southern hemisphere “anomalous” character. The values of electron density in the conditions of local

summer is greater than the values of local winter. And the heights of F2-layer in local summer are greater the heights in local winter.

In selected point of the southern hemisphere in the middle of June of local winter the sunrise time is about 8.6 LT, the sunset time – 16.7 LT. In the middle of December of local summer the Sun rises at $LT \approx 3.8$ and sets at $LT \approx 20.0$. In December the Sun doesn't disappear behind horizon approximately over 275 km.

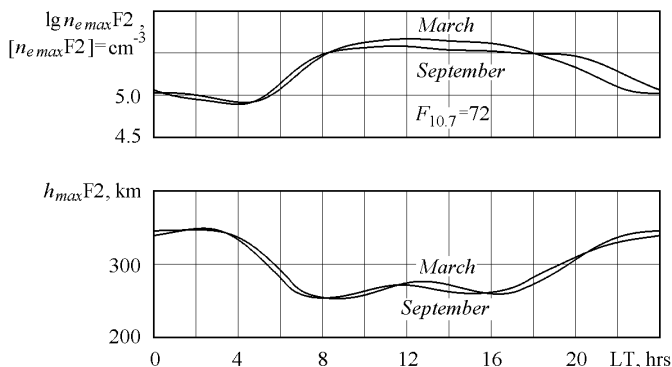


Fig. 14 – The spring and autumn variations of electron density and height of the F2-layer maximum

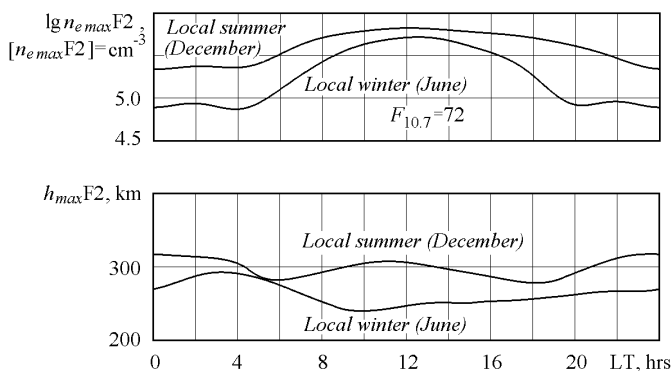


Fig. 15 – The daily variations $n_{e \max} F2$ and $h_{\max} F2$ in June and December in the southern hemisphere

The main feature of the variations of height $h_{\max} F2$ at mid-latitudes of the southern hemisphere is relatively small change of values during the day.

Development of ionospheric models by dates receiving by the incoherent scatter method in Institute of Ionosphere of NAS and MES of Ukraine. The creation of empirical model CCIR became possible due to the statistically provided data of a world network of vertical sounding stations. Though the incoherent scatter data are the most informative ones in a wide altitude range, but they have the regional limitations. In Institute of ionosphere in the eightieth years there was developed an empirical model of the daily courses of the altitude profiles of electron density, ion and electron temperature by the incoherent scatter date, presented in tabular form for the different seasons and levels of solar and geomagnetic activity (E. I. Grigorenko, S. V. Grinchenko, et al). Now M. V. Lyashenko develops CERIM IION Model (Central Europe Regional Ionospheric Model) which allows to calculate seasonal and daily courses of electron density, ion and electron temperatures of ions, vertical velocity of the plasma transport, as well as some parameters of dynamic and thermal processes in ionospheric plasma.

Conclusions. The results of CCIR model calculations confirm axial asymmetry of ionosphere. The CCIR model calculations clearly demonstrate the phenomena of seasonal and geographical anomalies. The daily courses of the parameters of F2-layer maximum ($h_{max}F2$ and $n_{e\ max}F2$) have characteristic anomalies too. In winter the daily course $n_{e\ max}F2$ has well expressed the Chapman form with one midday maximum; in summer the daily course $n_{e\ max}F2$ has two maxima (day and evening), and the summer amplitude of a daily course is less than winter one. At northern mid-latitudes the winter excess of electron density $n_{e\ max}F2$ of quiet ionosphere is observed approximately in the range of 9-17 LT. In the rest time of the day winter values $n_{e\ max}F2$ are less summer ones.

At increase of solar activity there is observed the increasing of $h_{max}F2$ and $n_{e\ max}F2$ during all time of days. The increase of $n_{e\ max}F2$ at increasing of solar activity is especially appreciable in winter daytime. Therefore, the effect of seasonal anomaly is more expressed at higher solar activity.

The spring and autumn values of electron density and height of F2 maximum are about the same.

References: 1. Jones W.B., Gallet R.M. Representation of diurnal and geographic variations of ionospheric data by numerical methods // Journal of Research of the National Bureau of Standard – D. Radio Propagation. – 1962. – Vol. 66D, № 4. – P. 419-438. 2. Jones W.B., Stewart F.G. A numerical method for global mapping of plasma frequency // Radio Sci. – 1970. – Vol. 5, № 50. – P. 773-784. 3. Brunini C., Conte J.F., Azpilicueta F., Bilitza D. A different method to update monthly median h_mF2 values // Adv. Space Res. – 2013. – Vol. 51. – P. 2322-2332. 4. Hoque M.M., Jakowski N. A new global model for the ionospheric F2 peak height for wave propagation // Ann. Geophysicae. – 2012. – Vol. 30. – P. 797-809. 5. Shubin V.N., Karpachev A.T., Tsybulya K.G. Global model of F2 layer peak height for low activity based on GPS radio-occultation data // J. Atm. Sol.-Terr. Phys. – 2013. – Vol. 104. – P. 106-115. 6. Rush C.M., PoKempner M., Anderson D.N., Stewart F.G., Perry J. Improving ionospheric maps using theoretically derived values of f_oF2 // Radio Sci. – 1984. – Vol. 18, № 1. – P. 95-107.

7. Rush C.M., PoKempner M., Anderson D.N., Perry J., Stewart F.G., Reasoner R.K. NTIA Report 84-140. Global Maps of f_oF_2 derived from observation and theoretical values // Institute for Telecommunication Sciences. National Telecommunications and Information Administration. US Department of commerce, 1984. – 144 p. 8. Bradley P.A. Mapping the critical frequency of the F2-Layer: Part I – requirements and developments to around 1980 // Adv. Space Res. – 1990 – Vol. 10, № 8. – P. 47-56. 9. Crane R.K. Evaluation of global and CCIR models for estimation of rain rate statistics // Radio Sci. – 1985. – Vol. 20, № 4. – P. 865-879. 10. ITU-R Reference ionospheric characteristics // Recommendation ITU-R P. 1239-3 (02/2012) – 29 p.

Received 08.08.2014

UDC 550.388.2

Seasonal anomaly in variations of global distributions of F2-layer electron density according to CCIR model / S. V. Grinchenko // Bulletin of NTU “KhPI”. Series: Radiophysics and ionosphere. – Kharkiv: NTU “KhPI”, 2014. – No. 47 (1089). – P. 74-91. Ref.: 10 titles.

Построены планетарные распределения электронной концентрации $n_{e\max}F_2$ и высоты $h_{\max}F_2$ главного максимума ионосферы. Проанализированы основные закономерности долготно-широтных вариаций этих параметров в северном и южном полушариях. Основное внимание уделено эффекту сезонной аномалии. Показано, что согласно расчётам по модели CCIR сезонная аномалия проявляется на широтах от 15° до 60° с. ш. примерно с 9 до 12 часов местного времени. В южном полушарии сезонная аномалия не наблюдается.

Ключевые слова: модель CCIR, IRI, модель NeQuick, планетарное распределение ионосферных параметров, географическая аномалия, сезонная аномалия, декабрьская аномалия, полугодовая аномалия, Visual Fortran.

Побудовано планетарні розподіли електронної концентрації $n_{e\max}F_2$ і висоти $h_{\max}F_2$ головного максимуму іоносфери. Проаналізовано основні закономірності довготно-широтних варіацій цих параметрів в північній і південній півкулях. Основна увага приділена ефекту сезонної аномалії. Показано, що згідно з розрахунками за моделлю CCIR сезонна аномалія проявляється на широтах від 15° до 60° пн. ш. приблизно з 9 до 12 години місцевого часу. У південній півкулі сезонна аномалія не спостерігається.

Ключові слова: модель CCIR, IRI, модель NeQuick, планетарний розподіл іоносферних параметрів, географічна аномалія, сезонна аномалія, груднева аномалія, піврічна аномалія, Visual Fortran.